PREDICTING FOREST ROAD SURFACE EROSION AND STORM RUNOFF FROM HIGH-ELEVATION SITES

J. M. Grace III

ABSTRACT. *Forest roads are a concern in management because they represent areas of elevated risks associated with soil erosion and storm runoff connectivity to stream systems. Storm runoff emanating from forest roads and their connectivity to downslope resources can be influenced by a myriad of factors, including storm characteristics, management practices, and the interaction of management practices and successive storm events. Mitigating sediment export and ensuring that storm runoff has negligible impacts on downstream resources requires a more complete understanding of forest road erosion and sediment delivery dynamics. Progress in the area of road and stream connectivity issues hinges on reliable prediction tools to inform broader-scale modeling of watershed-scale effects of forest roads and management practices. In this study, the Water Erosion Prediction Project (WEPP) model was evaluated based on the results from 156 runoff-generating storm events during a continuous five-year study of nine high-elevation road sections in the Appalachian Mountains. The model adequately predicted sediment yield from the road sections with an overall Nash-Sutcliffe model efficiency (E) of 0.76, Willmott refined index of agreement (d_r) of 0.56, percent error of 5%, and average storm difference (ASD) of 1.2 kg. In contrast, WEPP predictions of storm runoff were not as good, and the poor agreement was attributed to an inability to determine the source area for runoff from some of the larger runoff events. In general, the WEPP model for these high-elevation sites adequately described the sediment yield for the road sections.*

Keywords. *Forest roads, Long-term simulation, Runoff, Sediment, Water Erosion Modeling, WEPP.*

Forestlands typically have reduced soil erosion and sediment delivery to downslope ecosystems and water resources (Grace and Zarnoch, 2013; Neary et al., 2009; Yates and Sheridan, 1983) in comparison to most other land use categories. The storm runoff and eroded sediment yields exhibited by forested ecosystems have been documented by numerous investigations (Ford et al., 2011; Hood et al., 2002; Wynn et al., 2000), literature reviews (Grace, 2005a; Grace and Clinton, 2007; McNulty and Boggs, 2010), and synthesis reports (Jones et al. 2012; Joyce et al., 2009). Forest roads can cause accelerated soil erosion (Clinton and Vose, 2003; Grace, 2002a) and can be the dominant area of sediment yield from forestlands (Binkley and Brown, 1993). However, data directly linking upslope forest road erosion and sediment delivery to stream systems continue to be lacking. The bulk of the existing literature has estimated sediment delivery rates as a function of upslope erosion rates or failed to isolate forest roads (Grace, 2005b; Grace and Clinton, 2007). These facts, in addition to the scarcity of soil erosion data for forest roads, have been attributed to unsurfaced forest roads remaining an area of limited understanding and great concern in forest management. Consequently, the reliability of current soil erosion prediction technology to accurately model forest road erosion is relatively unknown in many geographic locations, including the high-elevation (>500 m above mean sea level) forests in the eastern U.S.

Design principles governing road storm runoff management and sediment control emphasize protecting the soil from raindrop impact, minimizing road density, minimizing storm runoff quantity through proper drainage, and locating roads at adequate distances from stream systems (Croke and Mockler, 2001; Grace, 2005b; Litschert and MacDonald, 2009; Sheridan and Noske, 2007). Manipulating any of the abovementioned factors directly influences storm runoff by altering either the energy required to detach sediment particles or the energy required to transport detached sediment, thereby influencing the degree of road connectivity to the streams. Steep slopes associated with higher-elevation sites are a road design challenge because storm runoff from steep slopes has increased energy to detach and transport sediment (elevation head in the energy equation), slopes often have multiple roads intercepting storm runoff flow paths (switchbacks to control gradients), and slopes increase the likelihood of direct connectivity (stream crossings from roads traversing slopes) (Grace, 2005a). The complex topography and engineering design aspects associated with these sites present unique water resource protection challenges in forest road management. Further exacerbating the situation is the fact that these watersheds are typically headwater watersheds, least impacted by anthropogenic influences, and are critical to surface drinking water supplies in the southeastern U.S. The potential risks or consequence of water resource

Submitted for review in November 2015 as manuscript number NRES 11646; approved for publication by the Natural Resources & Environmental Systems Community of ASABE in March 2017.

Mention of company or trade names is for description only and does not imply endorsement by the USDA. The USDA is an equal opportunity provider and employer.

The author is **Johnny McFero Grace III, ASABE Member,** General Engineer, Center for Forest Watershed Research, Southern Research Station, Florida A&M University, 1740 S. Martin Luther King Jr. Blvd., Perry-Paige Bldg., Suite 303 North, Tallahassee, FL 32301; phone: 850-412-7383; email: jmgrace@fs.fed.us.

impacts associated with road management in these critical watersheds may be magnified.

Models have proven beneficial in predicting field- and watershed-scale soil erosion and hydrology to aid in peak flow estimation, design of runoff and stream routing structures, design and implementation of systems to improve water management, and environmental impact evaluations of management and disturbance activities. In particular, properly calibrated soil erosion and hydrology models have been shown to be applicable as decision-making or decision-support tools in forest management for various geographic regions (Babbar-Semens et al., 2013; Flanagan et al., 2013; Laflen et al., 1991; Sun et al., 1998). One such physically based model, the Water Erosion Prediction Project (WEPP), can be applied to forested watersheds to simulate a wide range of conditions and scenarios for decision support. The reliability of WEPP, and other leading soil erosion prediction technologies, to accurately describe soil erosion and storm runoff generation processes is not well understood, primarily due to the lack of adequate field experimental data in high-elevation forests. Previous work indicates that the calibration and subsequent reliability of existing models are improved with the availability of sufficient input data for sensitive parameters and long-term observational data (Arnold et al., 2012; Flanagan et al., 2013; Renschler, 2003; USEPA, 2002).

Robust and reliable field experiment data from forest roads in high-elevation eastern forest settings can provide necessary input data to effectively evaluate the adequacy of the WEPP prediction technology. In this study, the objectives were to quantify the sediment yield from high-elevation unsurfaced forest road sections and estimate the sediment yield from road sections using WEPP. Specifically, observed individual storm soil erosion, storm runoff, and sediment yield from nine high-elevation forest road sections were compared to WEPP simulations to evaluate the adequacy of the WEPP prediction technology for the given scenarios. The aim was to use WEPP to adequately predict (model efficiency (E) > 0.80) sediment yield from the study road sections in high-elevation sites in the southern Appalachians for the observed storms. The specific objectives were to (1) calibrate WEPP for the nine high-elevation road sections; (2) determine the adequacy of soil erosion, sediment yield, and storm runoff WEPP model predictions; and (3) apply the GIS version of WEPP to illuminate the efficacy of forest watersheds in buffering local soil erosion at the watershed scale. Scientists, land managers, and policy makers require improved understanding and reliable prediction technology to adequately explain forest road erosion from high-elevation sites in eastern forests. The results of this study provide information on the applicability of WEPP in predicting erosion from high-elevation road sections typical of Appalachian mountain watersheds.

METHODS

STUDY AREA DESCRIPTION

The study area is located in northeast Georgia at approximately 35° N latitude and 83° W longitude. This area is within the Chattooga River District of the Chattahoochee National Forest and characteristic of the Appalachian mixed mesophytic forest, with overstory of primarily mixed broadleaf forest species (fig. 1). The overstory species in the area include oak (*Quercus* spp.), maple (*Acer* spp.), poplar (*Liriodendron tulipifera*), elm (*Ulmus* spp.), birch (*Betula* spp.), ash (*Fraxinus* spp.), hickory (*Carya* spp.), magnolia (*Magnolia* spp.), eastern hemlock (*Tsuga canadensis*), and pine (*Pinus* spp.). The understory consists of rhododendron (*Rhododendron* spp.) and mountain laurel (*Kalmia latifolia*). The temperate climate in the area is characteristic of the Central Appalachian Broadleaf Forest - Coniferous Forest - Meadow Province of the Appalachian-Cumberland Ecoregion (Bailey, 1980). Long-term average annual precipitation in the study area is 1800 mm, with 65% of this total occurring as rainfall. Soils are Hayesville series (fine, kaolinitic, mesic Typic Kanhapludults) surface soil overlaying clay loam subsoils (USDA-SCS, 1981). The study road is a benched crowned design, a design typically found in the Appalachian watersheds, traversing an area approximately 900 m above mean sea level, known as Patterson Gap. The road design, stormwater routing structures, study design, and monitoring procedures were described previously by Grace (2006, 2011).

EXPERIMENTAL DESIGN

The study randomly located three blocks, each with three road sections and lead-off ditch structures draining the sections, for a total of nine study road sections (fig. 2). Lead-off ditch structures, commonly referred to as turn-outs, are design features that convey and disperse road section storm runoff from the roadside ditch to the downslope forest buffer. The study employed two experimental designs to satisfy each of the two components of interest: (1) modeling the sediment yield and storm runoff from road sections, and (2) evaluating the trap efficiency of sediment control structures. The former experiment, reported here, used a nested design with three sections nested within three blocks along the study road to investigate soil erosion and storm runoff, and the latter experiment was previously reported (Grace and Elliot, 2011). The study road sections were originally defined and reconstructed with 3% to 5% gradients and road section lengths ranging from 40 to 60 m (table 1). Roadside ditching and lead-off ditch structures draining the study road sections were reconstructed at the initiation of the investigation during the summer of 2003 to ensure road drainage uniformity for the experimental sections. The road ditch specifications reconstructed or incorporated for the study consisted of a ditch depth of 0.33 m and 45° (1:1) sideslopes.

STORM EVENT MONITORING

Monitoring stations were installed in lead-off ditch structures for precise runoff measurement. Monitoring stations featured a 2.4 m trapezoidal approach section, a 0.33 m, 60° V, extra-large trapezoidal flume, a flowmeter, a submerged probe pressure transducer, and a storm runoff sampler (fig. 3). Storm runoff depths through the trapezoidal flume were measured continuously and logged at 5 min intervals using a flowmeter housed within the sampling station enclosure. Storm runoff discharge rate and volume were determined using the trapezoidal instantaneous flow level measurements in combination with the 60° V trapezoidal flume

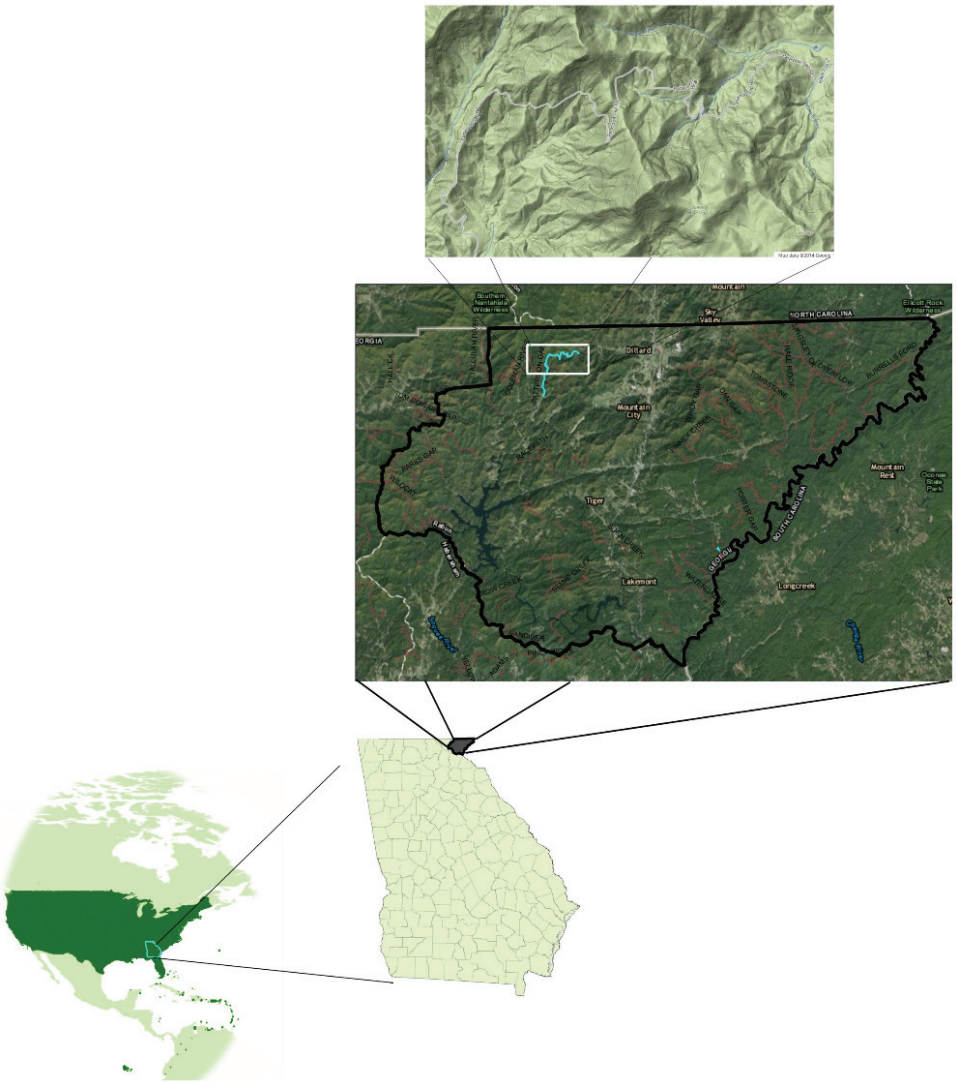

Figure 1. General location of the study road in Rabun County near Dillard, Georgia, in the Chattahoochee National Forest. Base map sources: USDA Forest Service and Google, 2011.

discharge equation (rating curve) internal to the flowmeter. Flow level (stage) was converted to flow with the following expression:

$$Q = 941.2H^{2.63} \quad (1)$$

where Q is the discharge rate from the flume (L s^{-1}), and H is the storm runoff hydraulic head (m).

Precipitation during the five-year study period (2003-2008) was monitored by a combination of recording tipping-bucket rain gauges and manual accumulating rain gauges. Precipitation was continuously monitored and recorded at 15 min intervals for the majority of storm events. However, a more detailed precipitation record was obtained for distinct periods during the investigation in order to explore the precipitation and runoff generation process in increased detail. The precipitation record was taken at 5 min intervals during these periods of intense data collection. Recorded precipitation and 15 min intensity at two on-site recording rain gauges (RRG1 and RRG3) were averaged to represent storm precipitation over the study period. Manual gauges (RG1, RG2, and RG3) were used for secondary precipitation quantification and to verify electronic records.

Precipitation events were defined as events resulting in a minimum of 0.5 mm of precipitation during a 6 h period. Storm runoff events were defined as events initiated by precipitation falling on at least one of the nine road cross-sections that resulted in at least 1 L of storm runoff at the flow monitoring and sampling stations. Sample collections in the investigation often were a combination of multiple precipitation and storm runoff events during the period covered by this study. Stormwater samplers sampled storm runoff by compositing a fraction of the stormwater flow stream into polypropylene bottles. Storm runoff collected for a given sampling period was subsampled by agitating the composited sample prior to the collection of a representative 500 mL grab sample. The grab samples were analyzed in the G.W. Andrews Forestry Sciences Water Laboratory in Auburn, Alabama, for total suspended solids (TSS) by gravimetric filtration (Method 2540D) (APHA, 1995). Sediment yield from road sections was determined as the product of TSS and the corresponding flow volumes for a given event.

Figure 2. Screen capture of the study road in Google Maps (Google, 2011) showing the topography with an overlay of blocks 1, 2, and 3 along Patterson Gap Road.

Table 1. Observed storm runoff, runoff coefficients, and sediment yield for the nine road sections in the investigation.

Road Section	Road Section Length (m)	Road Section Area (m^2)	Road Section Gradient (%)	Storm Runoff (mm)	Runoff Coefficient[a] (r_c, mm mm^{-1})	Sediment Load[b] (kg m^{-2})
A1	50	195	4	1096	0.26	6.3
A2	60	150	5	609	0.19	10.5
A3	40	85	4	380	0.10	12.1
B1	40	150	4	446	0.20	2.9
B2	40	120	5	561	0.23	5.8
B3	50	150	4	1476	0.12	0.3
C1	40	90	3	747	0.22	2.3
C2	50	150	3	680	0.33	1.6
C3	50	150	4	1781	0.25	1.9

[a] Runoff coefficient = observed storm runoff / observed precipitation.
[b] Sediment load = sediment yield at the road section drainage outlets for observed storms.

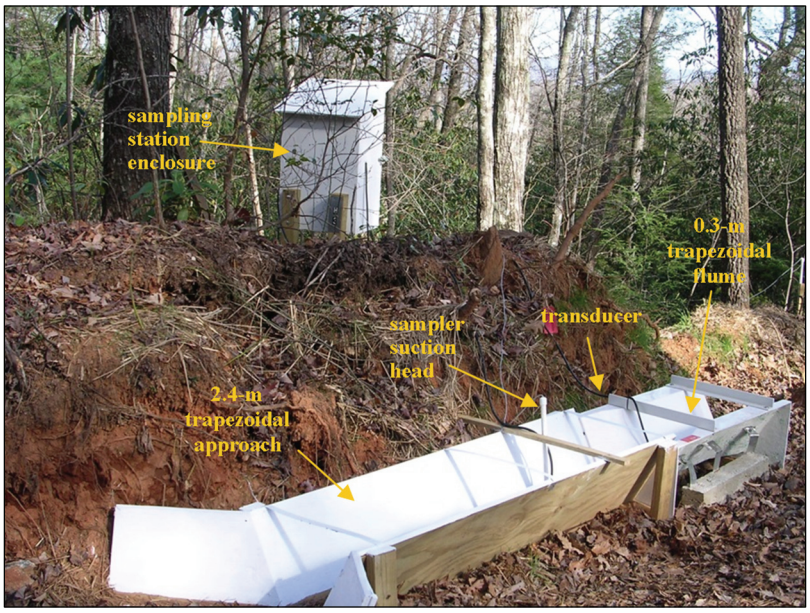

Figure 3. Typical flow routing structure located and monitoring station located at road section drainage structure outlets for flow quantification.

MODELING PROCEDURES

The WEPP model is a process-based, distributed parameter model developed by the USDA that can perform continuous simulations for water erosion predictions on a daily, monthly, or average annual basis (Flanagan and Nearing, 1995). The model predicts individual storm or daily soil erosion, sediment yield, and runoff from hillslopes and watersheds where Hortonian flow governs (i.e., precipitation rate exceeds infiltration

rate with negligible subsurface flow) based on climate, soils, management, and topography inputs. An attractive feature of the WEPP model, as opposed to competing models, is its primary use of the Mein and Larson (1973) modified Green-Ampt infiltration (GAML) for determination of rainfall excess and the modified kinematic wave model for hydrograph formulation. The model provides for the aggregation of single overland flow elements (OFEs) or areas with similar topography, soils, vegetation, and management into multiple OFEs that constitute a hillslope. Furthermore, in the watershed version, the model provides for the aggregation of multiple hillslopes with supporting channel networks. The abovementioned discretization is unique to WEPP and makes the model optimal for characterizing a typical road cross-section using OFEs to describe each component of the road cross-section (upslope contributing area, cutslope, road surface (with or without ditching), fillslope, and downslope receiving areas). The characterization of the study road sections for model calibration, validation, and testing purposes is presented in table 1. Individual input files were created in WEPP to characterize each slope, climate, soil, and management for the nine road sections monitored in this investigation. In the input file development, the study road sections were developed as single OFEs because the design theoretically isolated the road sections from the surrounding slopes, thereby eliminating offsite contributions to storm runoff. This simplified the modeling description by only considering the roadbed of the road section in the WEPP model. The assumption of a single OFE isolated from the surrounding slopes held during most storm events; however, in some storms, the assumption did not hold (detailed later in the discussion). The slope files were created based on ground elevation surveys conducted on the road sections during the study period. The climate file was an assimilation of individual storm events developed using the WEPP climate generator (CLIGEN, v. 5.3) based on precipitation characteristics observed at on-site recording rain gauges. Soil input files were created as Hayesville fine sandy loam road surface soils with varying degrees of gravel inclusion. An unrutted road surface with varying degrees of percent canopy cover and bulk densities of 1.8 to 2.3 g cm^{-3} was used to develop the management files for the road sections.

Model calibration is a critical phase in the modeling process in order to reduce the uncertainty in simulations, as reported by the general body of literature on the subject. The selection of data for the calibration phase of the modeling process hinged on several factors, including the quantity and range of data in the overall dataset, characteristics of storms within the dataset, data available for subsequent phases, and prior knowledge and expert judgement (Engel et al., 2007; Janssen and Heuberger, 1995; Moriasi et al., 2007). In general, the calibration relied on the selection of a representative set of data that considered the range of storms in the overall dataset to account for variability in the set to be modeled. Calibration was accomplished by selecting and simulating a representative sample of 12 storms, four storms from each of three predetermined storm size categories: small (0 to 41 mm), medium (42 to 65 mm), and large (66 to 114 mm). The 12 storms used in the calibration were a representative sampling of storms (5% to 10% sampling of storms) distributed within each of three predetermined storm size categories to cover the range of the data. Calibration focused on parameters in the soil and management input files because the two input files were expected to have the greatest influence on predictions based on previous literature (table 2). The model was manually calibrated following identification of the most sensitive input parameters, which were adjusted to optimize the fit (with the objective of maximizing test statistics) between the observed and predicted values. In particular, erodibility (K_i and K_r) and effective hydraulic conductivity (K_e) were the most sensitive calibration parameters in the soils input files, in the order presented in table 2. The management file parameterization focused on percent cover, initial soil roughness, and ridge height. Predictions were compared to determine the adequacy of the calibration by evaluating model goodness-of-fit statistics (Arnold et al., 2012).

Watershed-scale modeling was accomplished using the Online GIS interface version of WEPP Watersheds (WEPP OpenLayers 2011; http://milford.nserl.purdue.edu/ol/wepp/wepp1.php) (Cochrane and Flanagan, 2003; Flanagan et al., 2013) housed on the server at the National Soil Erosion Laboratory (NSERL). This GIS version of WEPP contains a web browser, Mapserver, and a Topographical Parameterization (TOPAZ) digital analysis tool to define a stream channel network and subsequently delineate a watershed to a defined outlet point (fig. 5) based on the U.S. Geological Survey (USGS) National Elevation Dataset's 30 m resolution digital elevation models (DEMs). In addition to the DEMs for slope file development, the model interfaced with the USGS National Land Cover Dataset for management file development, USDA Natural Resource Conservation Service (NRCS) SSURGO soils data for soil file development, and CLIGEN (v. 5.3) data parameterized for the Coweeta Hydrologic Laboratory weather station.

Data Analysis and Model Evaluation

Simulations were run for 156 storms observed during the five-year period of record for the road sections in the investigation. Predicted sediment yield and storm runoff resulting from simulated storms were recorded and tabulated for subsequent analysis. Observed and WEPP-predicted sediment yields and storm runoff were summarized for each of the study road sections for the study period. Road storm runoff and sediment yields were tested as a completely randomized design for significant road and block effects with general linear modeling (GLM) procedures using SAS software (SAS, 2004). The null hypothesis for the analysis of each dependent variable in the

Table 2. Selected soil and management input parameters and calibration ranges for WEPP model calibration.

Parameters	Units	Calibration Range in Modeling	Input Value
Interill erodibility (K_i)	kg s m^{-4}	1.00E+06 to 4.50E+06	2.50E+06
Rill erodibility (K_r)	s m^{-1}	2.50E-04 to 1.00E-03	1.00E-04
Effective hydraulic conductivity (K_e)	mm h^{-1}	0.0100 to 0.1000	0.0254
Initial saturation	%	30 to 60	40
Critical shear (t_c)	Pa	0.2000 to 0.3500	0.2045
Bulk density	g cm^3	1.8 to 2.3	2.1
Initial canopy cover	%	0 to 75	60
Percent rock	%	10 to 50	30
Albedo	unitless	0.50 to 0.65	0.60
Percent sand	%	-	30
Percent clay	%	-	30
Organic content	%	-	1.00E-03
Anisotropy ratio	unitless	-	25

investigation was that there were no block or section effects. Secondly, a regression analysis using SAS GLM procedures was performed on the data to test for differences in the observed and predicted yields by testing if the model slopes equaled 1 and intercepts equal zero (SAS, 2004). The three model evaluation statistics used to evaluate model performance were the Nash-Sutcliffe model efficiency, the refined Willmott index of agreement, and the coefficient of determination (Montgomery, 1991; Nash and Sutcliffe, 1970; Willmott et al., 2012). The coefficient of determination (r^2) is the square of the Pearson's correlation coefficient (r) and was used to describe the portion of the total variance in the observed sediment yield explained by the model. The value of r^2 ranges from 0 to 1, with a value closer to 1 indicating that a greater proportion of the total variance in observed sediment yield is explained by the model, i.e., better agreement (Legates and McCabe, 1999; Moriasi et al., 2007).

The Nash-Sutcliffe model efficiency (*E*; Nash and Sutcliffe, 1970) was used as the primary statistic to determine the goodness-of-fit for predicted sediment yields and was determined as:

$$E = 1 - \frac{\sum_{i=1}^{n}(Q_o i - Q_p i)^2}{\sum_{i=1}^{n}(Q_o i - \overline{Q}_o)^2} \quad (2)$$

where $Q_o i$ is the observed event sediment yield, $Q_p i$ is the predicted event sediment yield, $\overline{Q}_o$ is the mean of observed event sediment yield, and n is the number of observed values (n = 12 for calibration, and optimally n = 144 for validation). Similarly, the model efficiency was determined for event storm runoff predictions over the study period. The model performance in relation to E is given as: $E > 0.75$ (very good, also defined as "adequate" for this model evaluation), $0.65 < E \le 0.75$ (good), $0.50 < E \le 0.65$ (satisfactory), and $E \le 0.50$ (unsatisfactory) (Moriasi et al., 2007).

Historically, E has been used as a primary evaluation statistic for hydrologic model performance, with a range from negative infinity to 1 (Babbar-Sebens et al., 2013; Moriasi et al., 2007; Nash and Sutcliffe, 1970; Parajuli and Ouyang, 2013; Saleh et al., 2004, 2011). However, the potential challenges presented by oversensitivity to extreme values associated with goodness-of-fit measures that rely on squared differences have been noted (Legates and McCabe, 1999; Willmott et al., 1985, 2012). Willmott's refined index of agreement (d_r) was proposed to overcome challenges associated with sensitivity to outliers or extreme values and interpretability of the lower bounds of the original Willmott index. The form of d_r is given by:

$$d_r = \begin{cases} 1 - \dfrac{\sum_{i=1}^{n}|P_i - O_i|}{2\sum_{i=1}^{n}|O_i - \overline{O}|} & \text{when } \sum_{i=1}^{n}|P_i - O_i| \le 2\sum_{i=1}^{n}|O_i - \overline{O}| \\ \dfrac{2\sum_{i=1}^{n}|O_i - \overline{O}|}{\sum_{i=1}^{n}|P_i - O_i|} - 1 & \text{when } \sum_{i=1}^{n}|P_i - O_i| > 2\sum_{i=1}^{n}|O_i - \overline{O}| \end{cases} \quad (3)$$

where O_i is the observed data, P_i is the predicted data, $\overline{O}_o$ is the mean of observed data, and n is the number of observed values. The refined index is bound on the upper limit at 1 and on the lower limit at -1, which removes the interpretability challenges associated with the original Willmott index, which was unbound on the lower limit. The index provides the sum of the differences between the predicted and observed data relative to the sum of the magnitudes of the perfect model (Willmott et al., 2012). The index's interpretation is straightforward, with improved predictive ability or efficiency as the values approach the upper bound of 1. Values >0.5 are indicative of a model with increased predictive ability than the observed mean (Legates and McCabe, 2013; Willmott et al., 2012). Additionally, d_r of 0.5 indicates that the sum of the error magnitudes is about half that of the sum of the perfect model deviation and the observed deviation magnitudes. Similarly, d_r of 0 indicates equivalence of the sum of the error magnitudes and the sum of the perfect model deviation and the observed deviation magnitudes. In general, any values <0.5 are indicative of a model that has less predictive ability than the observed mean, and the value describes the level of inefficacy (Legates and McCabe, 2013).

RESULTS AND DISCUSSION

EVENTS AND PRECIPITATION CHARACTERISTICS

A total of 156 storm events initiated storm runoff from a minimum of one of the nine road sections during a five-year period from September 2003 to March 2008. Precipitation totaled 5000 mm for storm events observed during this period (fig. 4). Event precipitation depth was found to have a mean value of 32 mm and standard error of 3.1 mm. Precipitation intensities ranged from 0.3 to 80.0 mm h^{-1}, and the observed data showed that as much as 70% of the recorded intensities for the storms were at the lower end of the intensity range, with a mean value of 4.5 mm h^{-1}.

The calibration, validation, and testing phases of this modeling effort proved quite challenging due to the high variability in the precipitation characteristics during the period of study (table 3). The range of precipitation intensities was wide, with a minimum intensity of 0.4 mm h^{-1} and maximum intensity of 80.0 mm h^{-1}. However, the central tendency and relative prominence of sustained, lower-intensity storms for the study area during the period are indicated by the 11.7 h mean precipitation event duration and 4.5 mm h^{-1} intensity. The essentially narrow range of intensities made the selection of calibration storms exhibiting the full range of the data difficult (table 3). Representation of the full range of storms would have resulted in the inclusion of a sample of four large storms (>115 mm) associated with tropical systems. Consequently, two of these four storms were greater than the return period storm for the area and less than adequate representation of typical conditions. Inclusion of these events in the calibration storms would have only served to skew the calibration and subsequent predictions. The twelve storms used for model calibration exhibited a narrower range of amounts and intensities, which translated to a sample with reduced variability, as indicated in table 3. Further complicating the effort was a seasonal trend in the precipitation characteristics, as expected at high-elevation sites. In particular, the winter storm events were

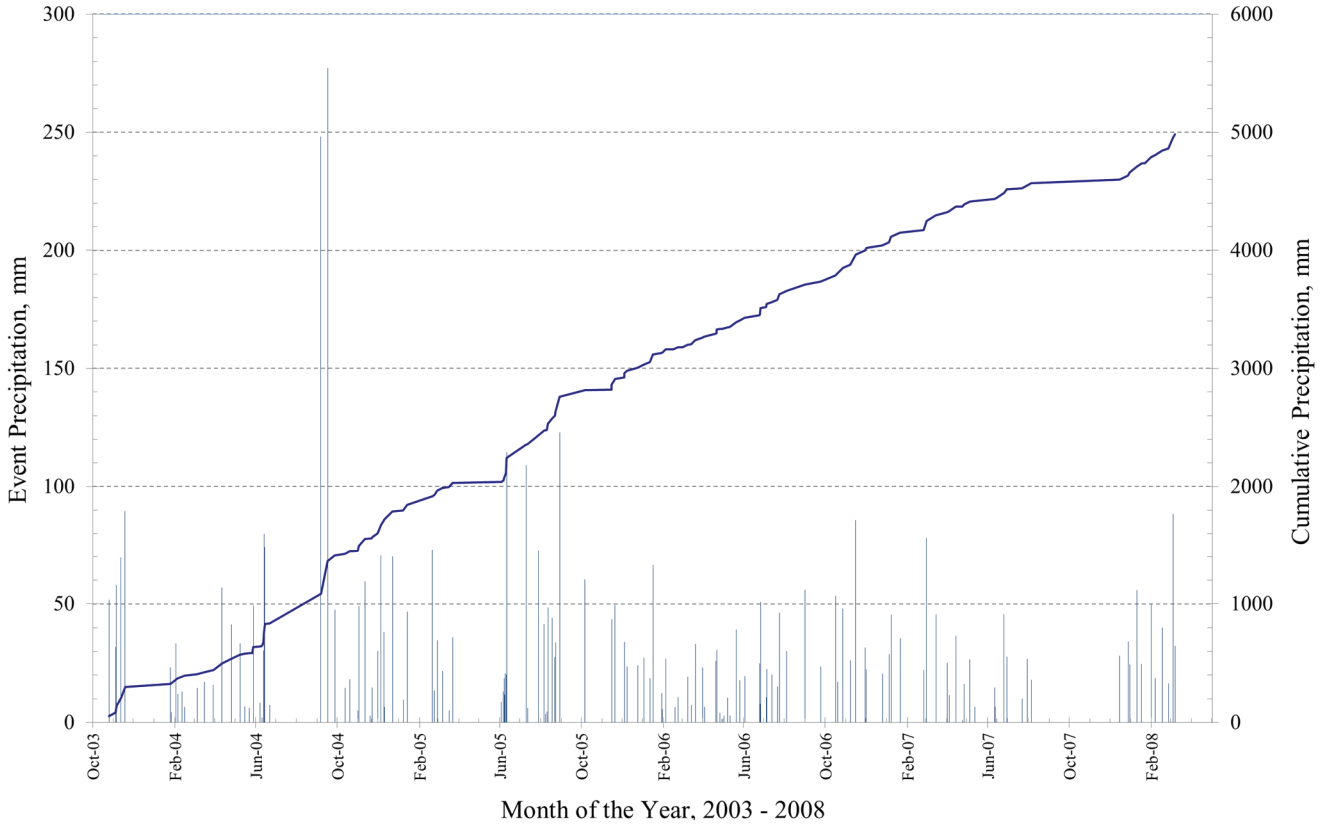

Figure 4. Observed precipitation at high-elevation sites in the Chattahoochee National Forest near Dillard, Georgia, during the study period.

Table 3. Computed statistics for the precipitation parameters based on observed data from the twelve calibration storms and overall dataset (population of storms during the study period) at the high-elevation sites near Dillard, Georgia, during the study period.

Parameter	Units	Mean	*N*	Standard Error	Standard Deviation	Sample Variance	Minimum	Maximum
Calibration storms								
Precipitation amount	mm	55.2	12	8.0	27.6	764.2	14.7	114.6
Overall dataset								
Precipitation amount	mm	32.8	140	3.1	36.5	1334.5	1.3	277.1
Intensity	mm h^{-1}	4.5	120	0.8	8.5	72.0	0.4	80.0
Duration	h	11.7	150	0.7	8.7	76.2	1.0	41.0
Time to maximum intensity	%	35.8	150	1.9	23.2	535.9	10.0	80.0

difficult to parameterize due to the extreme shifts in temperatures surrounding events and/or temperatures hovering around freezing, which presented problems with the instrumentation. Winter storm events typically resulted in temperatures that rose above freezing (0°C) for the duration of the precipitation and then quickly re-turned to below freezing at the conclusion of the precipitation event. The responsiveness of instrumentation, particularly submerged probe pressure transducers, often lagged that of the warming pattern and was not always optimal for accurate quantification of flow at the initiation of the storm runoff events.

Of the 156 storm events observed during the study, the number of storms simulated and used in this modeling ranged from 60 to 88 for each of the nine road sections. The potential number of storm events simulated differed from the actual number of storms recorded during the study period, primarily due to two reasons: no measurable quantity of sediment was observed, or observed runoff was in excess of the ability of the instruments to measure runoff from a study section. The latter reason is a result of areas outside of the road section contributing to storm runoff from the section. During several storms, the boundaries of the road sections were breached due to a couple of situations: high quantity and pulsed intensity storms resulting in "flashy" storm runoff events, and/or a combination of high antecedent moisture and high rainfall quantities. The flashy events were primarily isolated to the late spring and summer months, whereas the high antecedent moisture events were isolated to the winter and early spring months. As an example, events 22, 28, 29, 60, 62, 63, and 70 were summer storm events with greater than expected runoff coefficients for the majority of the road sections. These observed elevated runoff coefficients are primarily attributed to potential contributions from upslope areas outside of the delineated road section boundaries. To illustrate this phenomenon, figure 5 presents a delineation of the watershed using the USDA-ARS Topographic Parameterization Software (TOPAZ) analysis tool within the online WEPP GIS interface with an outlet just below block 3. This figure shows hillslope subcatchments with boundaries intersecting the study road and experimental road sections, which

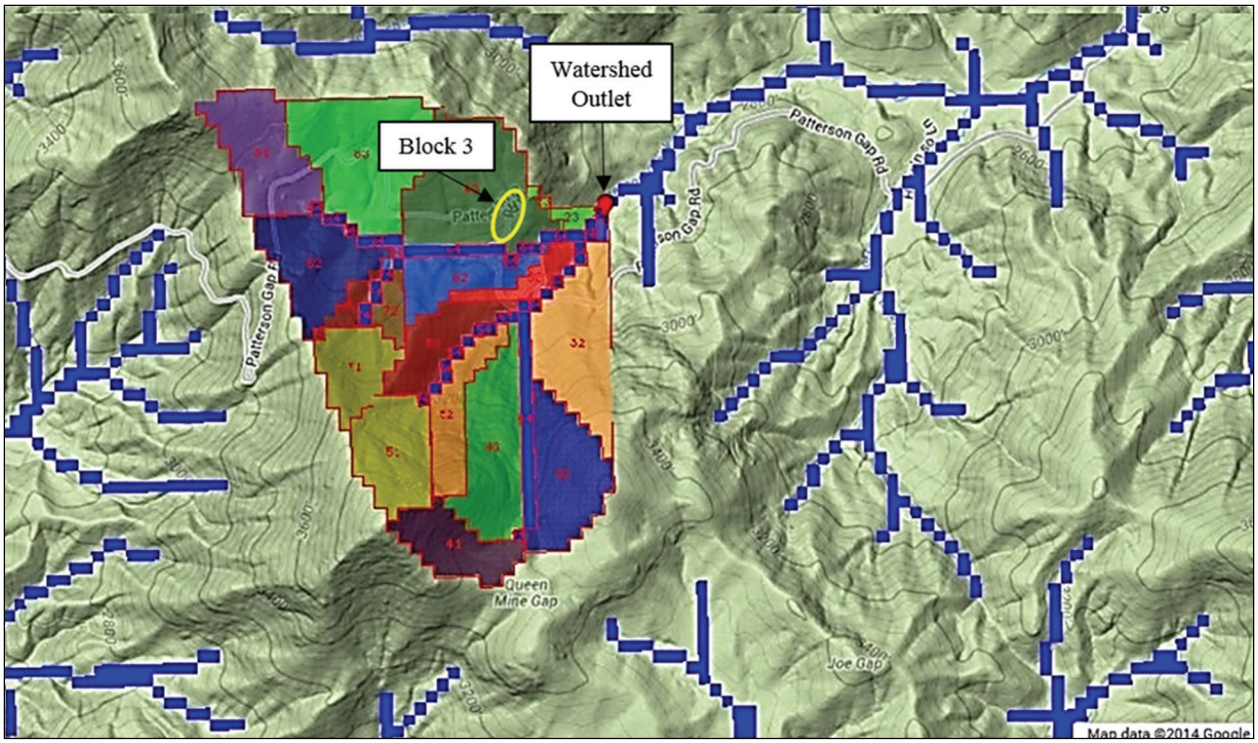

Figure 5. Depiction of a Patterson Gap watershed near Dillard, Georgia, and subcatchments as delineated by the TOPAZ analysis tool to an outlet point on the headwaters of Patterson Creek just east of road experimental block 3.

likely influenced storm runoff in the investigation. The intersections between the road and subcatchment boundaries are areas that likely had contributing areas that were outside of the road sections during events large enough to generate runoff to the forested hillslopes adjacent to the road plots. Events exhibiting storm runoff coefficients greater than 0.80 were excluded from the analysis because the only overland flow element that was considered in this model was that of the road section. The dynamics related to the contribution of upslope and subsurface runoff from the road sections during these events (hydrogeology) were beyond the scope of this article.

Storm Runoff Predictions

Predicted storm event runoff was plotted against observed storm runoff for each study block in the experiment and for the combined data for simulated storms along with the identity line (1:1 line) (fig. 6). The high variability in storm runoff production exhibited by the road sections is clearly reflected by these figures exhibiting low overall coefficients of determination (r^2). Overall, predicted and observed storm runoff agreement was poor, with r^2 values less than 0.30. Moderate agreement between predicted and observed storm runoff was found on block 1, which was the one exception of the three study blocks (fig. 6). The considerable scatter in the data indicates that much of the variability in the storm runoff data was poorly explained by the predicted storm runoff for the experimental road sections.

The poor agreement of the storm runoff component of the modeling effort can be seen in the tabulated comparisons of predicted and observed storm runoff over the study period (table 4). The *E* statistic ranged from -0.22 to 0.49, with an average of 0.15 for the road sections. Similarly, the d_r ranged from 0.49 to 0.72, indicating that the model ranged from no appreciable difference in predictive power over that of the observed mean to explaining less than half of the absolute-valued differences between the observations and the model predictions. The C3 section, with a storm runoff *E* of -0.22, average storm difference of 19.1 mm, and percent difference of -82%, clearly presented variability that was at the upper

Table 4. Predicted storm runoff, average storm difference, percent error, model efficiency, and Willmott refined index of agreement for experimental high-elevation road sections using the WEPP model.

Treatment	Observed Runoff (mm)	Predicted Runoff (mm)	Average Storm Difference (mm)	Percent Error (%)	Model Efficiency (*E*)	Willmott Refined Index of Agreement (d_r)
A1	1096	554	-13.1	-50%	0.14	0.69
A2	609	206	-6.8	-66%	0.22	0.49
A3	380	561	0.1	48%	0.49	0.71
B1	446	252	-5.8	-44%	-0.04	0.68
B2	561	604	0.9	8%	0.02	0.72
B3	1476	619	-8.9	-58%	0.35	0.70
C1	747	163	-16.2	-78%	0.03	0.49
C2	680	155	-9.4	-77%	0.38	0.65
C3	1781	315	-19.1	-82%	-0.22	0.49
Average	864	381	-8.7	-56%	0.15	0.62

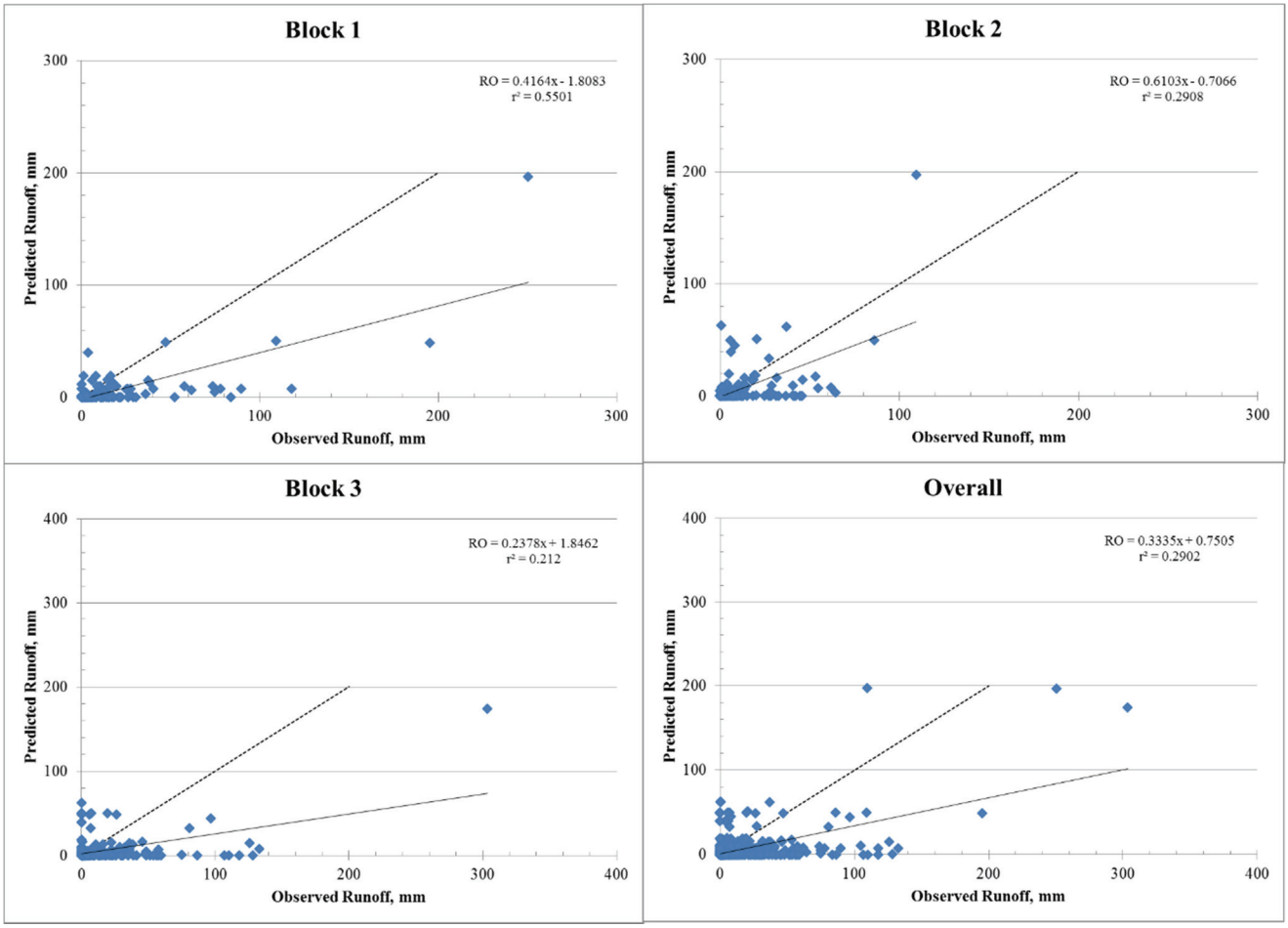

Figure 6. Graphical comparison of observed and WEPP-predicted storm runoff (mm) at the road section drainage outlet for each study block (blocks 1 through 3) and for all data combined (overall) for storm events at the high-elevation sites during the study period. The dashed identity line (1:1 line) represents perfect agreement between observed and predicted values.

range of the variability for all the sections. The negative *E* value for C3 (-0.22) corresponds to a d_r value of 0.49, which indicates that the sum of the error magnitudes is about half that of the sum of the perfect model and observed deviation magnitudes. The differences in the storm runoff *E* and d_r statistics for section C3 highlight the interpretability and oversensitivity challenges associated with *E* in situations presenting increased variability due to more extreme values. These low model performance values (*E* and d_r) coupled with the high percent errors and average storm differences found here indicate poor agreement and a considerable discrepancy between the simulated and observed values for the storm event runoff parameter over the study period. The relatively weak performance of the model for the storm runoff component may be attributed to the potential misrepresentations detailed above in the discussion of the calibration challenges. As mentioned above, some precipitation events may have resulted in the generation of excessively large runoff due to increased contributing area. Potential sources of errors in the runoff component presented here are consistent with those of Dun et al. (2013) in a watershed application of the WEPP model. In that study, the investigators presented precipitation events resulting in the production of observed storm runoff that was too great or too low as potential rea-sons for discrepancies in observed and predicted storm runoff.

Sediment Yield Predictions

Model simulation results for sediment yield are presented in table 5 along with summary statistics. WEPP-predicted sediment yield for the nine road sections over the study period averaged 667 kg for the simulated storms, whereas the observed sediment yield for the storms averaged 637 kg (table 5). Average percent error for the overprediction was 5%, which indicates that on average the model characterized sediment yield from the road sections. The errors for predictions of individual road section sediment yield had a wide range, with overpredictions as great as 164% for C3 and underpredictions as high as 62% for A3. This range could be expected considering the challenges associated with representing random variation in a deterministic model (Nearing, 1998) in combination with road section uniqueness in terms of spatial variability, soil property variability, storm variability, slope, aspect, maintenance history, trafficking history, and daylighting for the experimental road sections.

Model Goodness-of-Fit

The storm variations in predictions were explored by determining the differences between the predicted and observed sediment yields on an event-by-event basis. The average storm differences (ASD) in predicted sediment yield for road sections were within 9 kg of the observed sediment

Table 5. Predicted sediment yield, average storm difference, percent error, model efficiency, and Willmott refined index of agreement for experimental high-elevation road sections using the WEPP model.

Treatment	Observed Sediment Yield (kg)	Predicted Sediment Yield (kg)	Average Storm Difference (kg)	Percent Error (%)	Model Efficiency (E)	Willmott Refined Index of Agreement (d_r)
A1	1222	678	-6.5	-45%	0.82	0.60
A2	1579	1858	2.7	18%	0.89	0.63
A3	1021	387	-6.7	-62%	0.79	0.73
B1	432	257	-3.4	-41%	0.71	0.60
B2	692	1228	8.9	77%	0.66	0.47
B3	43	72	6.7	66%	-1.09	0.46
C1	211	321	2.4	52%	0.77	0.60
C2	243	440	2.7	82%	0.77	0.37
C3	290	765	4.2	164%	0.67	0.61
Average	637	667	1.2	5%	0.76[a]	0.56

[a] Section B3 was excluded in calculation of overall E.

yields for the simulated storms in the study. The underpredictions, on average, were within 7 (-7) kg of the observed yields for the storms over the entire simulation period. In contrast, the overpredictions were within 9 (+9) kg of the observed sediment yields over the entire study period. The overall average storm difference of +1.2 kg indicates an overprediction of sediment yield over the study with all sections considered. This difference represents a cumulative total difference of -270 kg in the sum of the event-by-event sediment yield differences between observed and predicted values.

WEPP-predicted sediment yields were regressed against observed sediment yields for the road sections in the investigation for 656 of the 1400 potential data points. The relatively low number (656) of regression points was the result of exclusion of regressions of zero values in observed and predicted data, missing data points, and data points influenced by contributing upslope areas outside the road sections. The relationship between predicted and observed sediment yields for road sections ranged from weak to strong as exhibited by the individual coefficients of determination (r^2), which ranged from 0.09 to 0.96 (fig. 7). On closer examination and analysis, some individual road sections and blocks were simulated better than others during the study. Simulated values for five of the nine road sections modeled here showed moderate to good agreement with observed sediment yields, with coefficients of determination of 0.74 or greater (fig. 7) and $p < 0.0001$. The slope of the best-fit linear

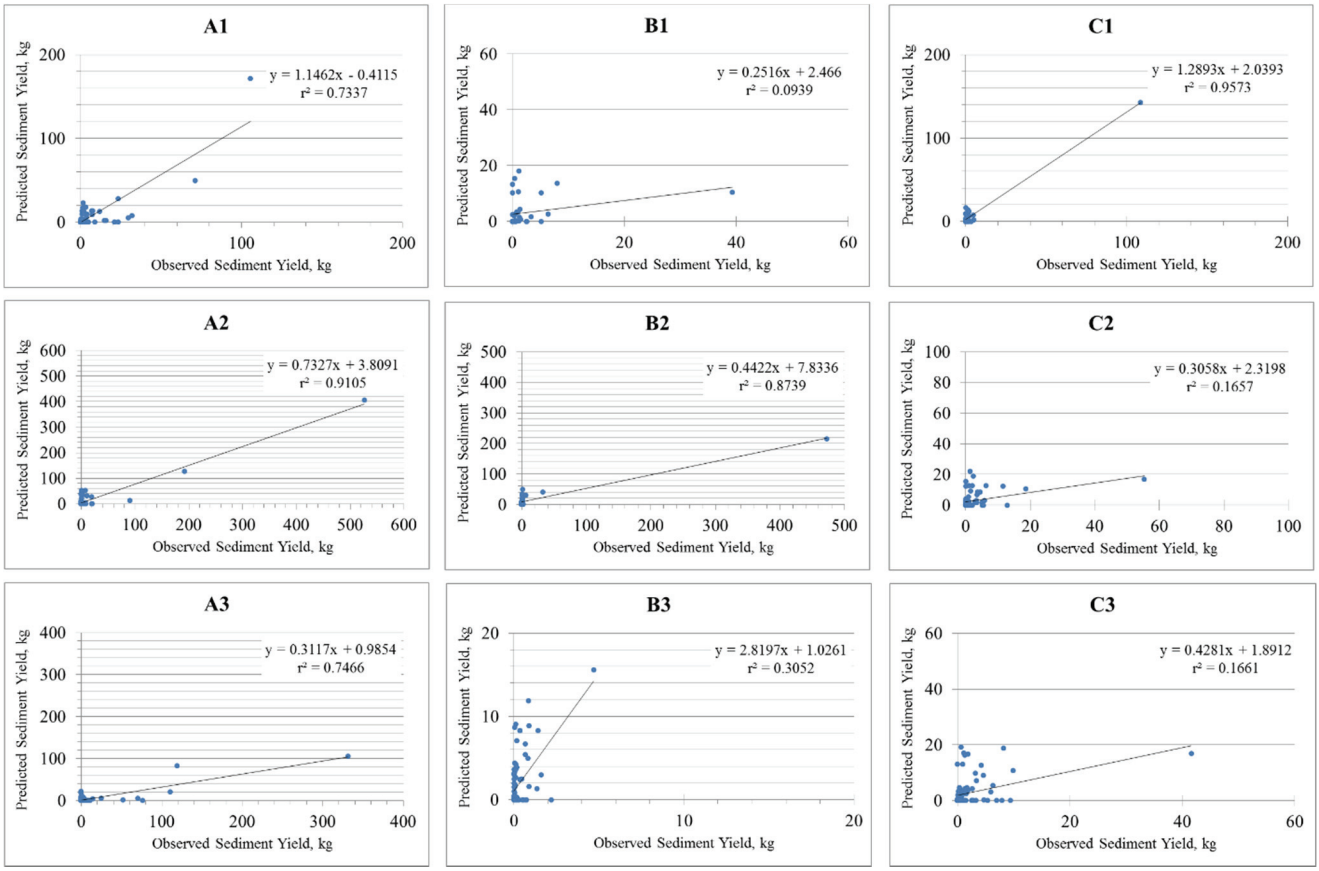

Figure 7. Graphical comparison of observed and predicted sediment yields (kg) at each road section drainage outlet for storm events at the high-elevation sites during the study period.

regression line for the road sections also showed a wide range, with a low slope value of 0.25 to a high of 2.8. It is important to note that the values at the extremes (0.25 to 0.31 on the low end of the slope range and 2.8 on the high end) were sections with weak correlations between predicted and observed values, with the exception of section A3. The simulated sediment yields for three of the road sections (B1, C2, and C3) indicated that the predicted values are only weakly correlated ($r^2 < 0.2$; p-values of 0.062, 0.0006, and <0.0001, respectively) with observed values. That is, the observed sediment yields from these particular road sections provide little information for predicting the values with all other parameters constant.

The plots of predicted versus observed sediment yield grouped by block exhibited moderate to good correlations for each of the blocks, with slopes of 1.15, 0.61, and 0.31 (fig. 8). In general, the predicted sediment yields from road sections in block 1 were in closer agreement with observed sediment yields than the road sections in blocks 2 and 3. This trend was supported by the increased deviation of the slopes of blocks 2 and 3 from unity, in comparison to block 1 with a slope of 1.15.

The observed data were analyzed as a mixed model using SAS MIXED procedures to evaluate the influence of road sections and blocks on sediment yields over the study period. In the analysis, blocks were fixed effects and road sections were considered random effects. The analysis of variance (ANOVA) failed to detect road section ($p = 0.2828$) or block effects ($p = 0.0729$) on the observed sediment yields. The plots of predicted sediment yield versus observed sediment yield shows a moderate correlation of 0.87 ($r^2 = 0.75$) (fig. 8). The slope of the relationship was 0.58, indicative of an underprediction. In general, the sediment yields were underpredicted by the WEPP model developed to characterize the road sections.

Model evaluation statistics for sediment yield from road sections in the investigation ranged from 0.66 to 0.89 and from 0.37 to 0.73 for E and d_r, respectively (table 5). The overall E for sediment yield was 0.76 with performance ratings described as good to very good (Moriasi et al., 2007; Parajuli and Ouyang, 2013) with the exception of one section (B3), which was excluded from the analysis. Section B3 had sediment yields that were highly variable, with overpredictions for the larger events (>30 mm) and underpredictions for smaller events (<30 mm). The sediment yield results for the section were indicative of an area with fluctuating boundaries and contributing area. The section was located at the toe of a curved slope, which likely contributed to the fluctuating boundaries from event to event. Theoretically, the roadbed was bisected by the crowned design, resulting in a contributing area boundary at the road crown. However, during larger events, the road surface runoff was great enough to overcome the elevation of the crown, resulting in an increased contributing area. The fact that the section was at the toe of a curve further complicated this problem.

In contrast to the E model evaluation results provided above, the d_r results were not as positive in this evaluation, with values ranging from 0.37 to 0.73. The performance of the model based on d_r for three of the sections (C2, B3, and B2) was unsatisfactory, with $d_r < 0.50$. The d_r values for the remaining road section predictions were >0.60, indicating that the model has the ability to explain the absolute differences between the observation and model predictions. The overall d_r for sediment yield of 0.56 indicates that overall the

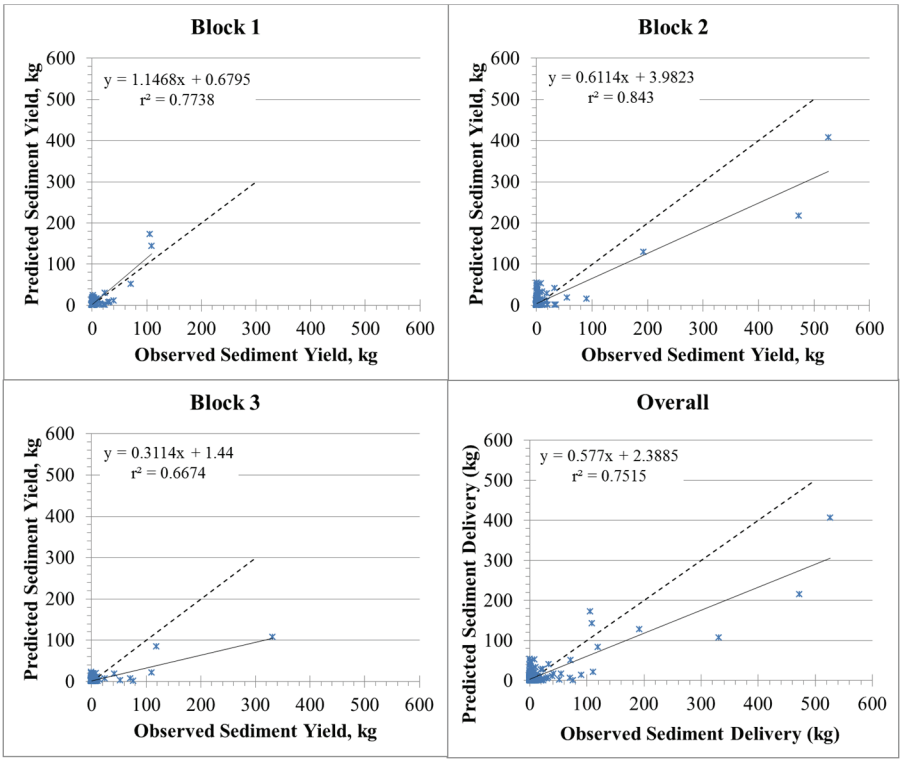

Figure 8. Graphical comparison of observed and WEPP-predicted sediment yields (kg) at road section drainage outlets for each study block (blocks 1 through 3) and for all data combined (overall) for storm events at the high-elevation sites during the study period. The dashed identity line (1:1 line) represents perfect agreement between observed and predicted values.

model has slightly more predictive ability than the observed mean, i.e., the model has some predictive ability. In general, the d_r values, though on the lower end of the range, indicate that the agreement between the predicted sediment yields and the observed yields is satisfactory.

Implications and WEPP Applications

With the adequacy of the calibrated WEPP model to predict sediment yields for the experimental road sections established using the observed data for the study road, longer-term predictions were attempted. In long-term (LT) (25-year) simulations of study road sections using climate data from the Coweeta Hydrologic Laboratory (12 km north of study area), sediment yield averaged 103 kg m^{-1} $year^{-1}$ for the nine experimental road sections. Average annual sediment yield per unit road length over the 25 years of simulation ranged from 55 to 150 kg m^{-1} $year^{-1}$ (fig. 9), which is well within the range previously reported of 20 to 500 kg m^{-1} $year^{-1}$ for high-elevation roads (Clinton and Vose, 2003; Reid and Dunne, 1984; Swift, 1984). The simulation results provided for a longer-term projection and analysis of sediment yield for the road sections in this investigation. The predicted sediment yield data were considered as a completely randomized design (CRD) with nine road sections subjected to 25 years of randomly generated climates. In contrast to the results of the analysis of the observed data, significant road section effects ($p < 0.0001$) were detected through the analysis of variance of the LT predicted yields per unit length based on the SAS general linear model used to describe the simulated yields over the 25-year period (SAS, 2004). The analysis revealed that predicted sediment yield per unit length of road was greatest for sections A2 and B2, as indicated by the Tukey grouping designations ($\alpha = 0.05$) above the chart columns for the sections (fig. 9). Similarly, sections C3 and B3 yielded the next greatest quantity of sediment on average over the 25-year simulated period, with section B3 detected as not significantly different from a section in the next grouping of sediment yields (C2). The analysis of long-term yields detected section A3 as yielding on average the least sediment over the 25-year period.

It should be noted that the predicted sediment yield at the outlet of individual road sections cannot necessarily be extrapolated to sediment yield at the watershed scale due to the myriad of erosion reduction attributes of forest watersheds (Grace, 2002b). This fact, as discussed in the previous section, is presented in the literature. One of the benefits of the research and data reported here is their value in characterizing small-scale elements and/or land use (overland flow elements in WEPP jargon) for broader-scale application in watershed-scale modeling. The Online GIS interface version of WEPP Watersheds (WEPP Openlayers 2011) was used to explore the observed LT simulations for the road sections in a broader context. An 85 ha watershed draining to a tributary of Patterson Creek was delineated with an outlet immediately east of experimental block 3 (fig. 5). The designated majority land use for the model simulation was mature forest (95%) with 18 hillslope subcatchments of varying areas ranging from 0.7 to 10.2 ha. The primary soil associations for the watershed were Tusquitee-Haywood and Saluda, representing 41% and 31% of the total watershed area, respectively. The WEPP model generated a soil erosion map depicting the soil erosion variation within the watershed, with pink catchments indicating higher soil losses (fig. 10). The 25-year average annual watershed sediment yield for the watershed was 2.5 tonne ha^{-1} $year^{-1}$ (209 tonne $year^{-1}$) observed at the watershed outlet, which represents 0.25 kg m^{-2} $year^{-1}$. The watershed delivery ratio, or predicted quantity of soil erosion within the delineated watershed that is delivered to the outlet, based on this modeling exercise was 0.942.

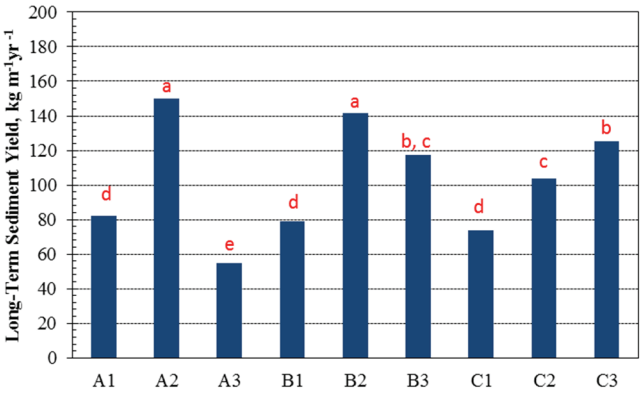

Figure 9. Long-term (25-year) average annual sediment yields at the road section drainage outlets for the experimental road sections as predicted by the WEPP hillslope model developed in this work. Sections with different Tukey grouping letters are significantly different at the 0.05 significance level.

The average sediment yield at the nine road section outlets of 103 kg m^{-1} $year^{-1}$ applied over the 1.8 km length and 5 m width of road that traversed the 85 ha watershed represents a sediment yield of 365 tonne $year^{-1}$. The watershed run presented here did not include sediment yield from roads (fig. 10), and the total sediment yield for the watershed, using the approach presented here, is the sum of the upland sediment yield of 209 tonne $year^{-1}$ plus the road sediment yield. Therefore, the total sediment yield for the watershed using this approach sums to 570 tonne $year^{-1}$. It should be noted that the road area in this watershed represents 1% of the total watershed area but represents 64% of the projected total yield and nearly twice (1.7 times) the sediment yield of the surrounding mature forest.

It should be noted that the analysis found that the conceptually geometrically isolated forest road sections were not necessarily isolated for all storm events during the study. In fact, for some road sections, the boundaries were breached on multiple occasions due to contributing areas outside the road cross-sections. Errors that may have resulted from the outside contributions were eliminated through the omission of the potentially troublesome data from the modeling exercise. It should be noted that these errors and the exclusion of these extreme field experimental data likely influenced the model performance, but the extent of this influence is unknown. Notwithstanding, the data and results of this study are expected to provide a clearer understanding of the potentially perpetual sediment yield capacity of active road cross-sections in high-elevation sites. The results suggest, and the literature supports, that sediment yield rates realized at road section outlets fail to translate to sediment yield at watershed outlets or sediment delivery to stream systems.

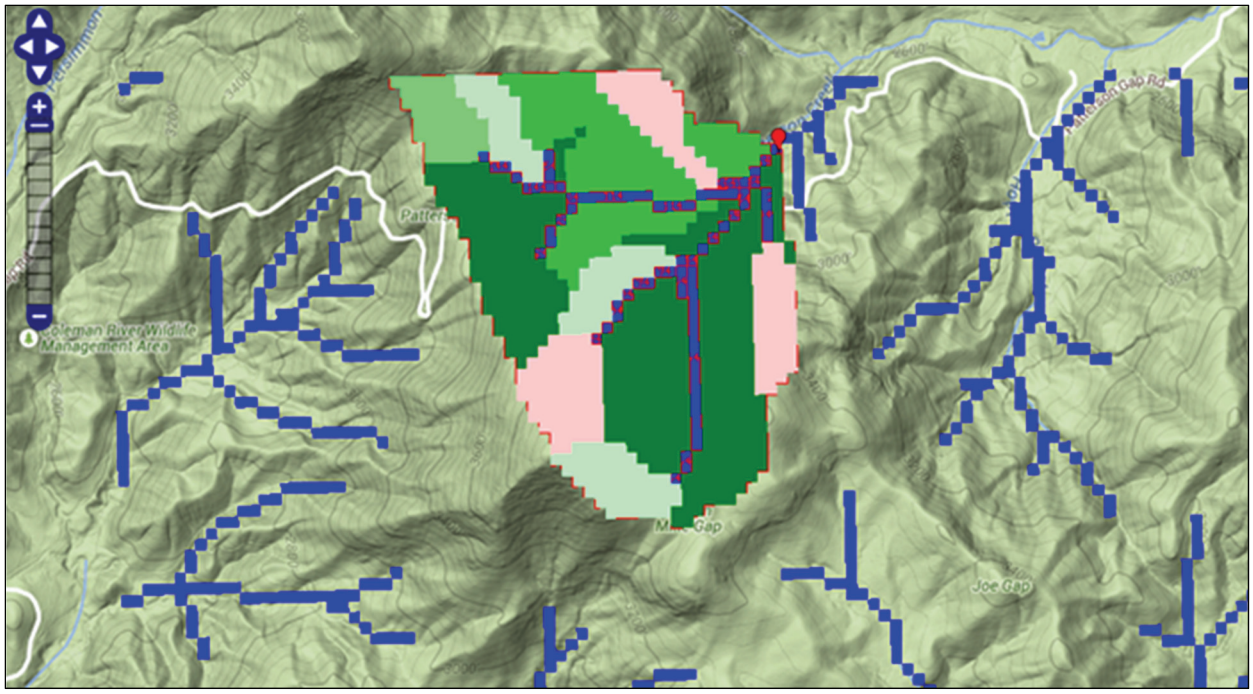

Figure 10. Soil erosion map depicting within-watershed erosion loss variation for the Patterson Gap watershed near Dillard, Georgia, with varying shades for subcatchments indicating different erosion rates. Pink indicates the upper range of soil erosion losses (4 to 8 tonne ha^{-1} year^{-1}), and dark green indicates the lower range of losses (0 to 1 tonne ha^{-1} year^{-1}).

Summary and Conclusions

In this investigation, soil erosion, sediment yield, and storm runoff results from a five-year forest road erosion experiment were examined with the goal of using the Water Erosion Prediction Project (WEPP) model to describe sediment yields from high-elevation road sections in the southern Appalachians. Storm runoff predictions were not well predicted, with overall poor agreement with observed values. In contrast, the experiment found no significant differences in sediment yield from road sections in the study, but this failure to detect differences was attributed to the high variability in the sediment yield from road sections over the study period. The predicted sediment yield results from experimental road sections were not significantly different from the observed sediment yield data based on the analysis of variance (ANOVA) results. The percent error of sediment predictions for individual road sections showed a wide range but had an aggregated sum of less than 10%, indicating adequate performance. The predicted values showed moderate to good correlations with observed sediment yields, with relatively small average storm differences and overall percent error. The primary test of model goodness-of-fit was the Nash-Sutcliffe efficiency coefficient, which was greater than 0.67 for all but one road section. The model efficiency coefficient was as high as 0.89 for one of the sections, indicating good agreement with observed sediment yield over the study period. The secondary model evaluation statistic, the Willmott refined index of agreement, yielded relatively low values but overall satisfactory model performance. In general, one conclusion drawn was that the single overland flow element (OFE) WEPP model detailed in this investigation for these high-elevation road sections adequately describes the sediment yield for the road sections during the study period (2003-2008).

Subsequently, long-term (25-year) WEPP simulations revealed that predicted sediment yields for the road sections differed significantly over the simulation period regardless of the precipitation and averaged 103 kg m^{-1} year^{-1} (or 43.2 kg m^{-2} for the 2.5 m width) for the nine road sections over the 25-year period of simulation. One would expect that on average the road sections would produce this quantity of sediment at the road section outlets annually. This illustrates the importance of sediment control best management practices (BMPs) at road drainage outlets to reduce sediment delivery potential. Note that the sediment yields and predictions from the single element models presented here are quite simplified and are likely not representative of the sediment yields that can be expected at a larger scale (watershed) that incorporates a more realistic range of soil, vegetation, geographic, and topographic detail. To elucidate this point, the Online GIS interface version of WEPP Watersheds (WEPP Openlayers 2011) was used to model an 85 ha watershed incorporating the study area. The predicted sediment yield at the watershed outlet was 209 tonne year^{-1}, which was only a fraction (57%) of that predicted at the road section outlets of 365 tonne year^{-1}. Looking at these yields on a per area basis, the watershed outlet yield of 0.25 kg m^{-2} year^{-1} represents only a fraction (<1%) of the 43.2 kg m^{-2} year^{-1} observed at the road section outlets.

The watershed modeling points to greatly reduced sediment yields and delivery rates due to the soil erosion reduction capacity of forest buffers and forest watersheds in general. In summary, this research seems to support previous investigations, which indicated that a more precise description of sediment dynamics in these systems may be required to refine or develop watershed (and broader scale) models to

assist in sustainable management of renewable resources and in provision of a robust suite of ecosystem services. Scientist, modelers, and managers are challenged here to seek and pursue forest road sediment yield and fate data in order to gain a better understanding and inform land managers and policy makers of the sediment dynamics of forest systems.

Acknowledgements

The author acknowledges the contribution and support efforts of the Chattahoochee-Oconee National Forests - Chattooga River (formerly Tallulah Ranger District) for providing research sites for the work, performing study-specific maintenance operations and grading, and administrative support over the life of the investigation. The author also wishes to acknowledge Preston Steele Jr., Engineering Technician with the USDA Forest Service Southern Research Station, for his subdaily response to assist with the arduous data collection and tireless efforts in stormwater sample analysis. Thanks are extended to the anonymous peer reviewers for their reviews and suggestions that were used to enhance the manuscript.

References

APHA. (1995). *Standard methods for the examination of water and wastewater* (19th ed.). A. D. Eaton, L. S. Clesceri, & A. E. Greenberg, Eds. New York, NY: American Public Health Association.

Arnold, J. G., Moriasi, D. N., Gassman, P. W., Abbaspour, K. C., White, M. J., Srinivasan, R., ... Jha, M. K. (2012). SWAT: Model use, calibration, and validation. *Trans. ASABE, 55*(4), 1491-1508. https://doi.org/10.13031/2013.42256

Babbar-Sebens, M., Barr, R. C., Tedesco, L. P., & Anderson, M. (2013). Spatial identification and optimization of upland wetlands in agricultural watersheds. *Ecol. Eng., 52*, 130-142. https://doi.org/10.1016/j.ecoleng.2012.12.085

Bailey, R. G. (1980). Description of the ecoregions of the United States. Misc. Publ. No. 1391. Washington, DC: USDA.

Binkley, D., & Brown, T. C. (1993). Forest practices as nonpoint sources of pollution in North America. *JAWRA, 29*(5), 729-740. https://doi.org/10.1111/j.1752-1688.1993.tb03233.x

Clinton, B. D., & Vose, J. M. (2003). Differences in surface water quality draining four road surface types in the Southern Appalachians. *South. J. Appl. For., 27*(2), 100-106.

Cochrane, T. A., & Flanagan, D. C. (2003). Representative hillslope methods for applying the WEPP model with DEMS and GIS. *Trans. ASAE, 46*(4), 1041-1049. https://doi.org/10.13031/2013.13966

Croke, J., & Mockler, S. (2001). Gully initiation and road-to-stream linkage in a forested catchment, southeastern Australia. *Earth Surf. Proc. Landforms, 26*(2), 205-217. https://doi.org/10.1002/1096-9837(200102)26:2<205::AID-ESP168>3.0.CO;2-G

Dun, S., Wu, J. Q., Elliot, W. J., Frankenberger, J. R., Flanagan, D. C., & McCool, D. K. (2013). Applying online WEPP to assess forest watershed hydrology. *Trans. ASABE, 56*(2), 581-590. https://doi.org/10.13031/2013.42689

Engel, B., Storm, D., White, M., Arnold, J., & Arabi, M. (2007). A hydrologic/water quality model application protocol. *JAWRA, 43*(5), 1223-1236. https://doi.org/10.1111/j.1752-1688.2007.00105.x

Flanagan, D. C., Frankenberger, J. R., Cochrane, T. A., Renschler, C. S., & Elliot, W.J. (2013). Geospatial application of the Water Erosion Prediction Project (WEPP) model. *Trans. ASABE, 56*(2), 591-601. https://doi.org/10.13031/2013.42681

Flanagan, D. C., & Nearing, M. A. (1995). USDA Water Erosion Prediction Project: Hillslope profile and watershed model documentation. NSERL Report No. 10. Washington, DC: USDA.

Ford, C. R., Laseter, S. H., Swank, W. T., & Vose, J. M. (2011). Can forest management be used to sustain water-based ecosystem services in the face of climate change? *Ecol. Appl., 21*(6), 2049-2067. https://doi.org/10.1890/10-2246.1

Google. (2011). Google Maps. Retrieved from https://developers.google.com/maps/

Grace III, J. M. (2002a). Effectiveness of vegetation in erosion control from forest road sideslopes. *Trans. ASAE, 45*(3), 681-685. https://doi.org/10.13031/2013.8832

Grace III, J. M. (2002b). Control of sediment export from the forest road prism. *Trans. ASAE, 45*(4), 1127-1132. https://doi.org/10.13031/2013.9913

Grace III, J. M. (2005a). Forest operations and water quality in the south. *Trans. ASAE, 48*(2), 871-880. https://doi.org/10.13031/2013.18295

Grace III, J. M. (2005b). Factors influencing sediment plume development from forest roads. *Proc. Environ. Connection Conf. 36* (pp. 221-230). Denver, CO: International Erosion Control Association.

Grace III, J. M. (2006). A new design to evaluate erosion and sediment control from forest roads. *Proc. Environ. Connection Conf. 37* (pp. 153-162). Denver, CO: International Erosion Control Association.

Grace III, J. M. (2011). Trap efficiency for road storm runoff detention in Southern Appalachian watersheds. *Proc. Intl. Symp. Erosion and Landscape Evolution.* St. Joseph, MI: ASABE.

Grace III, J. M., & Clinton, B. D. (2007). Protecting soil and water in forest road management. *Trans. ASABE, 50*(5), 1579-1584. https://doi.org/10.13031/2013.23969

Grace III, J. M., & Elliot, W. J. (2011). Influence of forest roads and BMPs on soil erosion. ASABE Paper No. 1110633. St. Joseph, MI: ASABE.

Grace III, J. M., & Zarnoch, S. J. (2013). Influence of forest road buffer zones on sediment transport in the Southern Appalachian region. *Proc. 15th Biennial Southern Silvicultural Research Conf.* (pp. 487-493). Asheville, NC: USDA Forest Service, Southern Research Station.

Hood, S. M., Zedaker, S. M., Aust, W. M., & Smith, D. W. (2002). Soil erosion in Appalachian hardwoods: Using the Universal Soil Loss Equation (USLE) to compare the impacts of different harvest methods. *North. J. Appl. For., 19*(2), 53-58.

Janssen, P. H. M., & Heuberger, P. S. (1995). Calibration of process-oriented models. *Ecol. Model., 83*(1), 55-66. http://dx.doi.org/10.1016/0304-3800(95)00084-9

Jones, J. A., Creed, I. F., Hatcher, K. L., Warren, R. J., Adams, M. B., Benson, M. H., ... Williams, M. W. (2012). Ecosystem processes and human influences regulate streamflow response to climate change at long-term ecological research sites. *BioScience, 62*(4), 390-404. https://doi.org/10.1525/bio.2012.62.4.10

Joyce, L. A., Blate, G. M., McNulty, S. G., Millar, C. I., Moser, S., Neilson, R. P., & Peterson, D. L. (2009). Managing for multiple resources under climate change: National forests. *Environ. Mgmt., 44*(6), 1022. https://doi.org/10.1007/s00267-009-9324-6

Laflen, J. M., Lane, L. J., & Foster, G. R. (1991). WEPP: A new generation of erosion prediction technology. *J. Soil Water Cons., 46*(1), 34-38.

Legates, D. R., & McCabe Jr., G. J. (1999). Evaluating the use of "goodness-of-fit" measures in hydrologic and hydroclimatic model validation. *Water Resour. Res., 35*(1), 233-241.

https://doi.org/10.1029/1998WR900018
Legates, D. R., & McCabe Jr., G. J. (2013). A refined index of model performance: A rejoinder. *Intl. J. Climatol., 33*(4), 1053-1056. https://doi.org/10.1002/joc.3487
Litschert, S. E., & MacDonald, L. H. (2009). Frequency and characteristics of sediment delivery pathways from forest harvest units to streams. *Forest Ecol. Mgmt., 259*(2), 143-150. https://doi.org/10.1016/j.foreco.2009.09.038
McNulty, S. G., & Boggs, J. L. (2010). A conceptual framework: Redefining forest soil's critical acid loads under a changing climate. *Environ. Pollut., 158*(6), 2053-2058. https://doi.org/10.1016/j.envpol.2009.11.028
Mein, R. G., & Larson, C. L. (1973). Modeling infiltration during a steady rain. *Water Resour. Res., 9*(2), 384-394. https://doi.org/10.1029/WR009i002p00384
Montgomery, D. C. (1991). *Design and analysis of experiments* (3rd ed.). New York, NY: John Wiley & Sons.
Moriasi, D. N., Arnold, J. G., Van Liew, M. W., Bingner, R. L., Harmel, R. D., & Veith, T. L. (2007). Model evaluation guidelines for systematic quantification of accuracy in watershed simulations. *Trans. ASABE, 50*(3), 885-900. https://doi.org/10.13031/2013.23153
Nash, J. E., & Sutcliffe, J. V. (1970). River flow forecasting through conceptual models: Part I. A discussion of principles. *J. Hydrol., 10*(3), 282-290. http://dx.doi.org/10.1016/0022-1694(70)90255-6
Nearing, M. A. (1998). Why soil erosion models overpredict small soil losses and under-predict large soil losses. *Catena, 32*(1), 15-22. https://doi.org/10.1016/S0341-8162(97)00052-0
Neary, D. G., Ice, G. G., & Jackson, C. R. (2009). Linkages between forest soils and water quality and quantity. *Forest Ecol. Mgmt., 258*(10), 2269-2281. https://doi.org/10.1016/j.foreco.2009.05.027
Parajuli, P. B., & Ouyang, Y. (2013). Chapter 3: Watershed-scale hydrological modeling methods and applications. In Dr. P. Bradley (Ed.), *Current perspectives in contaminant hydrology and water resources sustainability.* Rijeka, Croatia: InTech. https://doi.org/10.5772/53596
Reid, L. M., & Dunne, T. (1984). Sediment production from forest road surfaces. *Water Resour. Res., 20*(11), 1753-1761. https://doi.org/10.1029/WR020i011p01753
Renschler, C. S. (2003). Designing geo-spatial interfaces to scale process models: The GeoWEPP approach. *Hydrol. Proc., 17*(5), 1005-1017. https://doi.org/10.1002/hyp.1177
Saleh, A., Gallego, O., Osei, E., Lal, H., Gross, C., McKinney, S., & Cover, H. (2011). Nutrient Tracking Tool: A user-friendly tool for calculating nutrient reductions for water quality trading. *J. Soil Water Cons., 66*(6), 400-410. https://doi.org/10.2489/jswc.66.6.400
Saleh, A., Williams, J. R., Wood, J. C., Hauch, L. M., & Blackburn, W. H. (2004). Application of APEX for forestry. *Trans. ASAE, 47*(3), 751-765. https://doi.org/10.13031/2013.16107
SAS. (2004). SAS Online Doc. 9.1.3. Cary, NC: SAS Institute.
Sheridan, G. J., & Noske, P. J. (2007). Catchment-scale contribution of forest roads to stream exports of sediment, phosphorus, and nitrogen. *Hydrol. Proc., 21*(23), 3107-3122. https://doi.org/10.1002/hyp.6531
Sun, G., Riekerk, H., & Comerford, N. B. (1998). Modeling the hydrologic impacts of forest harvesting on Florida flatwoods. *JAWRA, 34*(4), 843-854. https://doi.org/10.1111/j.1752-1688.1998.tb01520.x
Swift, L. W. (1984). Gravel and grass surfacing reduces soil loss from mountain roads. *Forest Sci., 30*(3), 657-670.
USDA-SCS. (1981). Soil survey of Rabun and Towns counties Georgia. Washington, DC: USDA Soil Conservation Service. Retrieved from https://www.nrcs.usda.gov/Internet/FSE_MANUSCRIPTS/georgia/GA651/0/rabun.pdf
USEPA. (2002). Guidance for quality assurance project plans for modeling. EPA QA/G-5M. Report EPA/240/R-02/007. Washington, DC: U.S. Environmental Protection Agency, Office of Environmental Information.
Willmott, C. J., Ackleson, S. G., Davis, R. E., Feddema, J. J., Klink, K. M., Legates, D. R., ... Rowe, C. M. (1985). Statistics for the evaluation and comparison of models. *J. Geophys. Res. Oceans, 90*(C5), 8995-9005. https://doi.org/10.1029/JC090iC05p08995
Willmott, C. J., Robeson, S. M., & Matsuura, K. (2012). A refined index of model performance. *Intl. J. Climatol., 32*(13), 2088-2094. https://doi.org/10.1002/joc.2419
Wynn, T. M., Mostaghimi, S., Frazee, J. W., McClellan, P. W., Shaffer, R. M., & Aust, W. M. (2000). Effects of forest harvesting best management practices on surface water quality in the Virginia coastal plain. *Trans. ASAE, 43*(4), 927-936. https://doi.org/10.13031/2013.2989
Yates, P., & Sheridan, J. M. (1983). Estimating the effectiveness of vegetated floodplains/wetlands as nitrate-nitrite and orthophosphorus filters. *Agric. Ecosyst. Environ., 9*(3), 303-314. http://dx.doi.org/10.1016/0167-8809(83)90104-4